

Mechanism of Mobility Improvement of a-Si TFT with Channel Passivated Layer

Yasuo TANAKA, Ken TSUTSUI, Toshiko KOIZUMI†,
Hideaki YAMAMOTO and Toshihisa TSUKADA

Central Research Laboratory, Hitachi, Ltd.,

† Musashino Works, Hitachi Device, Ltd.,

Kokubunji, Tokyo 185, Japan

The a-Si TFT with the channel-passivated layer shows high mobility and low threshold-voltage compared with the conventional TFT. The β_{\max}^{-1} vs. channel-length relations indicate the existence of the induced n-channel under the drain/channel-passivation overlap region for $V_g < V_d$. The induced-channel shortens the effective channel-length to increase the observed mobility, and that suppresses the hole-injection from drain-electrode in $V_g < 0V$. Optimizing the conditions of depositing a-Si(i) layer, the off-current at $V_g = -20V$ decreases lower than $10^{-13}A$.

1. Introduction

The a-Si TFT's have been widely used in active-matrix liquid crystal displays (LCD's) [1]. The requirements of a-Si TFT's for TFT/LCD's are high on-current for signal-charging, low off-current (I_{off}) for signal-holding [2], low threshold-voltage (V_t) for reducing driving voltage and small V_t -shift for reliability [3]. Several types of structures have been proposed on the a-Si TFT's, so far. The inverted-gate-staggered a-Si TFT with the channel-passivated (CHP) layer has advantages of high mobility [4] and low off-current. However, it is not always clear why the CHP-TFT has these merits. Recently, the overlap-effects of CHP-TFT's were calculated using two-dimensional computer simulations [5]. We studied experimentally some ambiguous points to estimate the mobility (μ), the V_t and the I_{off} in the CHP-TFT's. Such conditions as the applied-voltages on the gate (V_g) and drain electrodes (V_d), the sizes of channel-width (W) and length (L) after fabrication, and the edge-effects should be taken into account carefully. In this paper, we will discuss the mechanism of the mobility increase and the V_t reduction, and the

conditions to lower off-currents in the CHP-TFT's.

2. Experiment

2.1 TFT Fabrication

Fig. 1 shows the cross-sectional view of an asymmetrical CHP-TFT in which the overlap-lengths of source/CHP and drain/CHP are made asymmetrically. On a glass substrate, a gate-electrode of Cr was formed, on which a gate-insulator of SiN (300 nm thickness), an undoped a-Si(i) layer (20 ~ 50 nm) and a CHP layer of SiN (200 nm) is continuously deposited by the rf (13.56 MHz) glow-discharge CVD method. The $\text{SiH}_4\text{-NH}_3\text{-N}_2$ mixtures were used for the depositions of the gate-insulator and the CHP layer, the pure SiH_4 was used for the a-Si(i) layer. The a-Si(i) layer degradation were prevented by controlling deposition temperature of the a-Si(i) and CHP layer. After the CHP patterns were formed, a light etch was necessary over the a-Si(i) surface by a diluted $\text{HF-NH}_4\text{F}$ buffer-solution to improve the source and drain contacts. Then, an a-Si(n^+) layer (30 nm) was deposited by the same CVD method using the $\text{SiH}_4\text{-H}_2\text{-PH}_3$ mixtures. The a-Si(n^+) layer

on the CHP layer was removed after the formation of source-drain electrodes of evaporated Cr and Al. Finally, a passivation layer was formed (not shown in Fig. 1).

2.2 Measurement

First, the overlap-effects of drain-electrode over the CHP layer on the CHP-TFT is investigated by comparison with the conventional inverted-gate-staggered TFT in which an a-Si(n^+) layer is deposited continuously on an a-Si(i) layer. We define the channel-length under the CHP layer as L , and the drain/CHP overlap-length as ΔOL . The μ and β values are derived from the differential curves of the $\sqrt{I_d}$ vs. V_g curves using the relation of $\sqrt{I_d} = \sqrt{(\beta/2) \cdot (V_g - V_t)}$, where $\beta = \mu \cdot C_{SiN} \cdot W/L$, I_d is the drain-current, and C_{SiN} is the capacitance of the SiN gate-insulator per unit area. In those curves, we define the maximum values of β and μ as β_{max} and μ_{max} , respectively. The $V_{t,max}$ and $V_{g,max}$ correspond to those maximum values using the relations of $\sqrt{I_d} = \sqrt{(\beta_{max}/2) \cdot (V_{g,max} - V_{t,max})}$ and $\beta_{max} = \mu_{max} \cdot C_{SiN} \cdot W/L$.

3. Results and Discussion

3.1 Dependences of μ and V_t on gate-voltage

Fig. 2 shows the μ vs. V_g and V_t vs. V_g characteristics for the CHP-TFT ($L = 10.1 \mu m$, \circ plots) and for the conventional TFT ($L = 11.5 \mu m$, Δ plots). Fig. 2 indicates that the mobility of the CHP-TFT has the large dependence on the gate-voltage, and has the maximum values ($\mu_{max} = 0.92 \text{ cm}^2/\text{V}\cdot\text{s}$, $V_{t,max} = 1.2 \text{ V}$) at around $V_g = 5 \text{ V}$ ($V_{g,max}$). The μ -values at a gate-voltage higher than 10 V are similar to those of the conventional TFT. On the contrary, the conventional TFT has a moderate peak in mobility at around 10 V ($\mu_{max} = 0.54 \text{ cm}^2/\text{V}\cdot\text{s}$, $V_{t,max} = 2.6 \text{ V}$). The CHP-TFT's have higher μ_{max} -values and lower $V_{t,max}$ -values than those of the conventional TFT's in the range of $V_g < V_d$.

3.2 Effects of the drain/CHP overlap region

Fig. 3 shows the β_{max}^{-1} vs. L characteristics of the asymmetrical CHP-TFT in which ΔOL is large ($\Delta OL = 4.8 \mu m$, \circ plots), compared with those of the same TFT with the source and drain electrodes exchanged, i.e., ΔOL is small ($\Delta OL = 0.0 \mu m$, \square plots). It is clear that the plots corresponding to the large ΔOL (\circ plots) and the small ΔOL (\square plots) are on the separate lines. On the other hand, as for the symmetrical CHP-TFT shown in Fig. 4, these phenomena have not been observed, and the both lines are exactly matched each other. In Fig. 4, ΔOL is almost the same, i.e., one side is $\Delta OL = 1.7 \mu m$, \circ plots, another side is $\Delta OL = 1.5 \mu m$, \square plots. If we use the channel-length L' which is equal to $L - \Delta OL$ instead of the channel-length L shown in Fig. 1, then the line of the $\Delta OL = 4.8 \mu m$ (\circ plots) shifts to the left, and the line after the correction (\bullet plots) is the same as the line corresponding to the $\Delta OL = 0.0 \mu m$ (\square plots). This fact suggests that the existence of the induced n-channel under the ΔOL region shown in Fig. 1, and this dominates the drain-current characteristics in the low gate-voltage of $V_g < V_d$. Then the channel length L becomes shorter by ΔOL , and as a result, the observed mobility increases.

After the correction of the ΔOL -effect (\bullet plots) in Fig. 2, the μ_{max} -value of the CHP-TFT takes a lower value ($\mu_{max} = 0.73 \text{ cm}^2/\text{V}\cdot\text{s}$) than the original value ($0.92 \text{ cm}^2/\text{V}\cdot\text{s}$), but this value is still higher than that of the conventional TFT ($0.54 \text{ cm}^2/\text{V}\cdot\text{s}$). That was mainly caused by the differences of the edge-effects of the drain-electrode in the CHP-TFT and the plasma-damages on a-Si(i) back-surface in the conventional TFT.

Fig. 5 (a) and (b) show the comparison of the μ vs. V_g characteristics of different ΔOL , i.e., (a) $\Delta OL = 1.4 \mu m$ and (b) $\Delta OL = 0.3 \mu m$ for different V_d . Fig. 5 (a) shows the typical μ vs. V_g curves of the CHP-TFT, while Fig. 5

(b) shows similar to those of the conventional TFT. The induced n-channel under the Δ OL region has the effect of accelerating the rise of on-current as well as shortening channel-length, and going with this, the $V_{t,max}$ -values become lower as shown in Fig. 2 and Fig. 5.

3.3 Off-current of the CHP-TFT's

Discussing the off-current of a-Si TFT, we should distinguish the two types of off-currents. One has the dependence on V_g due to the rising of the hole-current, another has not the dependence on V_g due to simple leakage currents such as the surface or boundary leakage current. In the conventional TFT's, it is difficult to achieve the off-currents lower than 10^{-13} A at $V_g = -20$ V and $V_d = 10$ V, although it is easier to achieve at $V_g = -5$ V. Because, the conventional TFT's have a strong electric field around the edge of drain electrode and the hole-injection easily occur. However, the CHP-TFT's have a weak electric field under the drain-electrode due to the electrical shield-effect of the Δ OL region. Moreover, the induced n-channel of the Δ OL region blocks the hole-injection from drain-electrode under negative gate bias. Consequently, the hole-injection in the CHP-TFT's will be suppressed lower level than the conventional TFT. Fig. 6 shows the dependence of the I_{off} -values at $V_g = -20$ V on deposition temperature of a-Si(i) layer. As was expected, the I_{off} -value is kept lower than 10^{-13} A in the range lower than 230°C . However, in the range higher than 240°C , the I_{off} -value increases exponentially with the deposition temperature of a-Si(i) layer. This fact is explained as follows: the increase of acceptor levels in a-Si(i) layer due to the hydrogen release from this layer makes easy the hole-injection from the a-Si(n^+) layer under drain-electrode. In Fig. 6, the influence of channel-length on off-current is relatively small. Thus, the off-currents of CHP-TFT's are

lowered with the optimized a-Si(i) layer.

This condition is also useful to prevent the abnormal positive V_t -shift accompanied with moderating of the rise of on-current under the negative-stress.

4. Summary

The a-Si TFT with the channel-passivated layer show high mobility and low threshold-voltage compared with the conventional TFT's. The on-current for the CHP-TFT's has the dependence on the drain/CHP overlap-length Δ OL, and indicate the existence of the induced n-channel under the Δ OL region in the low gate-voltage of $V_g < V_d$. The induced n-channel shortens the effective channel length to increase the observed mobility, and accelerates the rise of mobility in the low gate-voltage region. Another effect of the induced n-channel is suppressing hole-injection from the drain electrode under negative gate-voltage. The off-currents of the CHP-TFT's are reduced to a level lower than 10^{-13} A at $V_g = -20$ V with the optimized a-Si(i) layer.

ACKNOWLEDGEMENTS

The authors would like to thank Mr. H. Matsumaru and Mr. M. Yamaguchi for their technical discussions and support. We gratefully acknowledge the encouragement and support from Dr. H. Matsumura of Central Research Laboratory, Hitachi, Ltd. and Dr. A. Sasano of Mobara Works, Hitachi, Ltd.

REFERENCES

- [1] F. Inoue et al.: SID'88 DIGEST(1988), 318.
- [2] Y. Kaneko et al.: IEEE Trans. Electron Devices, 36(1989), 2953.
- [3] Y. Kaneko et al.: Extended Abstracts of the 18th Intn'l Conf. on Solid State Devices and Materials(1986), 699.
- [4] S. Hotta et al.: SID'86 DIGEST(1986), 296.
- [5] J. G. Shaw and M. Hack: J. Appl. Phys., 65(1989), 2124.

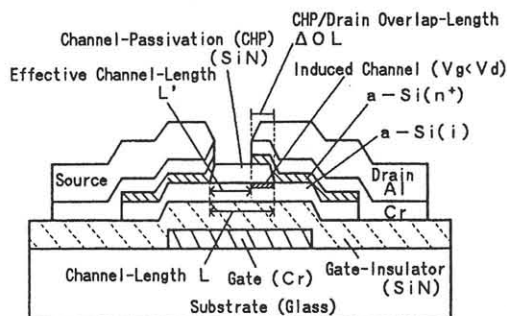


Fig. 1 Cross-sectional view of the asymmetrical CHP-TFT, with an overlap region of the drain-electrode on the channel-passivated layer.

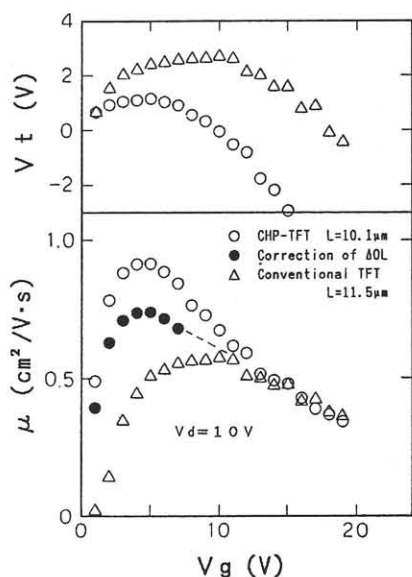


Fig. 2 μ and V_t vs. V_g characteristics of the symmetrical CHP-TFT (\circ) with the correction of ΔOL effect (\bullet), compared with those of the conventional TFT (Δ).

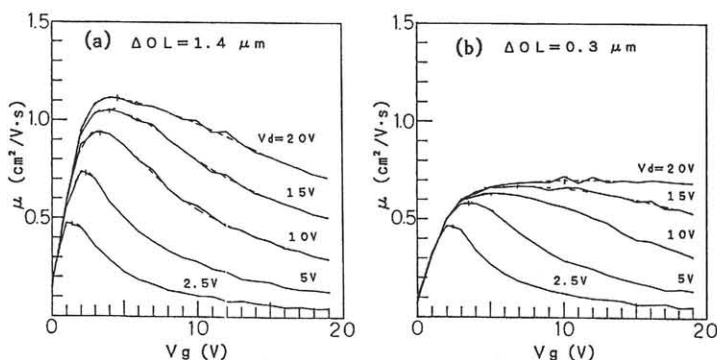


Fig. 5 Comparison of μ vs. V_g characteristics of different ΔOL , (a) $\Delta OL = 1.4 \mu m$ and (b) $\Delta OL = 0.3 \mu m$ for different V_d .

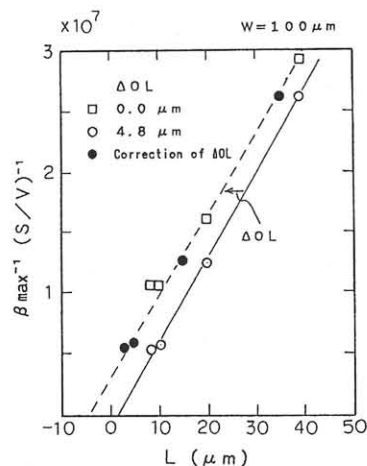


Fig. 3 β_{max}^{-1} vs. L characteristics of the asymmetrical CHP-TFT ($\Delta OL = 4.8 \mu m$, \circ) with the correction of the ΔOL effect (\bullet), compared with those of the same TFT with the source and drain electrodes exchanged ($\Delta OL = 0.0 \mu m$, \square).

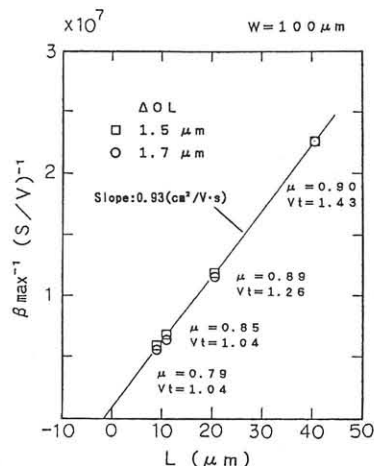


Fig. 4 β_{max}^{-1} vs. L characteristics of the symmetrical CHP-TFT ($\Delta OL = 1.7 \mu m$, \circ) compared with those of the same TFT with the source and drain electrodes exchanged ($\Delta OL = 1.5 \mu m$, \square).

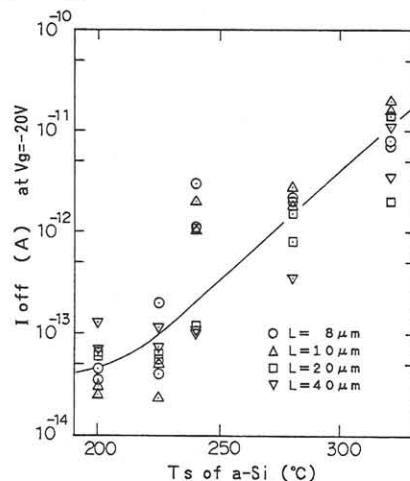


Fig. 6 Dependence of I_{off} at $V_g = -20 V$ on the deposition temperature of a-Si(i) layer.